Preprints.org

Article

Titanium-Biohybrid Middle Ear Prostheses: A Preliminary In Vitro Study

Mario Mosconi , Elena Carlotto [*] , Laura Caliogna , Micaela Berni , Giulia Gastaldi , Michele Conti , Alice Maria Brancato , Valentina Bina , Domenico Minervini , Stefano Malpede , Anna Chiara Stellato , Francesco Lazzerini , Luca Bruschini , Marco Benazzo , Pietro Canzi

Article

Titanium-Biohybrid Middle Ear Prostheses: A Preliminary In Vitro Study

Mario Mosconi [1,2], **Elena Carlotto** [3,*], **Laura Caliogna** [2], **Micaela Berni** [2], **Giulia Gastaldi** [4,5], **Michele Conti** [6], **Alice Maria Brancato** [2], **Valentina Bina** [4], **Domenico Minervini** [3], **Stefano Malpede** [3], **Anna Chiara Stellato** [3], **Francesco Lazzerini** [7], **Luca Bruschini** [7], **Marco Benazzo** [1,3] **and Pietro Canzi** [1,3]

1   Department of Clinical, Surgical, Diagnostic and Pediatric Sciences, University of Pavia, Pavia, Italy
2   Orthopedics and Traumatology Clinic, IRCCS Policlinico San Matteo Foundation, 27100 Pavia, Italy
3   Department of Otorhinolaryngology, University of Pavia, IRCCS Policlinico San Matteo Foundation, Viale Camillo Golgi, 19, 27100, Pavia, Italy
4   Department of Molecular Medicine, University of Pavia, 27100 Pavia, Italy
5   Centre for Health Technologies, University of Pavia, 27100 Pavia, Italy
6   Department of Civil Engineering and Architecture (DICAr), University of Pavia, Via Ferrata 3, 27100, Pavia, Italy
7   Otolaryngology, ENT Audiology and Phoniatrics Unit, University Hospital of Pisa, Pisa, Italy.
*   Correspondence: e.carlotto.ec@gmail.com; Tel.: +39.338-2191252

Abstract: Tissue bioengineering has been assuming a pivotal role in implementing alternatives to conventional ossicular middle ear replacement prostheses to overcome extrusion while preserving acoustic properties. This in vitro study aims to explore for the first time in current literature the feasibility of a biohybrid middle ear prosthesis composed of titanium surrounded by bone extracellular matrix as bio-coating. We have hereby studied the adhesion and proliferation of human adipose-derived mesenchymal stem cells (hASC) on titanium scaffolds in vitro. Moreover, we identified the osteogenic differentiation of hASC using immunofluorescence assay to analyze osteoblasts gene expression profile (Alp, Runx2, Col1a1, Osx, and Bglap) and we accounted the presence of collagen as a marker of hASC ability to secrete extracellular matrix. We utilized scanning electron microscopy to evaluate the presence of extracellular matrix on the scaffolds. Our preliminary data demonstrated the titanium ability to support human adipose-derived mesenchymal stem cell colonization, proliferation, and osteoblastic differentiation, to obtain a biohybrid device. Our experience seems encouraging, we advocate further in vivo research to corroborate our results towards bone transplantation.

Keywords: middle ear; ossicular replacement prosthesis; titanium; bone transplantation; tissue engineering; hearing loss

1. Introduction

Ossiculoplasty is a well-established surgical procedure intended to restore appropriate sound-wave transmission from the tympanic membrane to the stapes footplate via a reconstructed ossicular chain [1]. It often represents the final stage of reconstruction after eradication of various middle ear (ME) pathologies including chronic otitis media, adhesive otitis media, atelectasis, tympanosclerosis, tumors, traumatic injuries, and congenital diseases- which may damage the chain, leading to conductive hearing loss [2]. The ideal ossiculoplasty material should ensure hearing restoration, be safe and steadily inbuilt into surrounding tissues. Autologous incus interposition grafting remains one of the reconstruction techniques of choice, with rare extrusion and cost savings. Unfortunately, the availability and quality of patients' incus are often limited in diseased ears [1]. Several kinds of synthetic prostheses, such as metals, ceramics, plastics, and composites, are now commercially available for both partial (PORP) and total ossicular replacement prostheses (TORP). Titanium has been used in ossicular reconstruction since the early 1990s, demonstrating to be a satisfactory material in terms of hearing results and easy surgical manipulation [3]. However, also titanium prostheses

present downsides due to early and late postoperative extrusion. A recent meta-analysis reports extrusion rates of 9% for the PORP cohorts and 15.65% for the TORP cohorts [4]. In recent years new possible tissue bioengineering options have been explored to overcome extrusion risks [5,6]. However, to the best of the authors' knowledge, no bioengineering studies exist that employ conventional titanium prostheses combined with biological material coating. In this in vitro study, we analyzed the capability of titanium to support human adipose-derived mesenchymal stem cells (hASC) colonization, proliferation, and osteoblastic differentiation. We aim at proposing ossicular transplantation to obtain biohybrid prostheses made up of titanium surrounded by bone extracellular as bio-coating, here we present our preliminary results.

2. Materials and Methods

2.1. Production of titanium-biohybrid middle ear prostheses

Scaffolds. The scaffolds used in this *in vitro* study were the titanium prostheses commonly used in our otosurgical department and gifted by Gyrus ACMI®. The construct (Micron TM All Titanium PORP® and TORP®) was made of titanium (Ti6A4V ELI), and it has a size range of 2-5 mm (Figure 1).
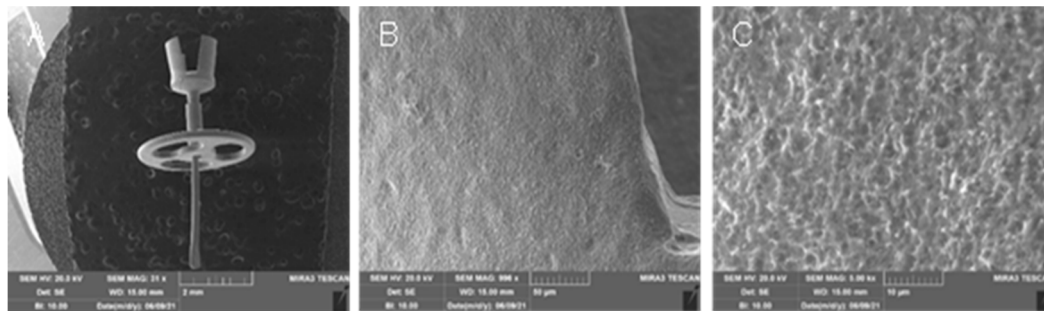
Figure 1. SEM study of the prosthesis utilized. A, the structure shape of the prosthesis (mag. 31x). B and C, higher magnification s show the surface roughness (mag. 900x and 5.00 kx, respectively).

Extraction of human adipose-derived stem cells (hASCs). Subcutaneous adipose tissue was obtained from the peritrochanteric region of healthy donors during hip replacement surgery. Informed consent was obtained from all patients before surgery. The study was conducted according to the 1975 Declaration of Helsinki, and approved by the Ethics Committee of San Matteo Foundation, Research and Care Institute, Pavia, Italy (P-20190023312, 9 April 2019). The samples preserved in sterile conditions were taken to the laboratory for processing. At the laboratory, the finely minced tissue was incubated in a digestion buffer (0.01% collagenase type II in DMEM F12-HAM medium) for 1 h at 37 °C in a shaking water bath [7]. At the end of the incubation time, the collagenase was neutralized, and the suspension was filtered (100 mm) and centrifuged at 1200 rpm for 10 min at 4 °C. The pellet containing the hASCs was washed twice with PBS, treated with lysis solution, and finally suspended in growth medium (GM, DMEM F12-HAM supplemented with 10% FBS, 100 U/mL penicillin, 100 μg/mL streptomycin, and 0.25 μg/mL amphotericin). The hASCs seeded in 75 cm² polystyrene flasks were cultured in GM up to 95% confluence in a humidified atmosphere of 95% air with 5% CO2 at 37 °C. The adherent cells were trypsinized with Trypsin EDTA, and 5000 hASCs/cm² tissue culture plates were seeded in a new flask [8]. These passages were repeated three times. At the third passage, the hASCs were positive for the mesenchymal stem cell markers CD73, CD90, and CD105 and negative for the hematopoietic cell markers CD34 and CD45, according to the analysis performed by flow cytometer (Navios Beckman Coulter). Data were acquired, displayed, and elaborated by Kaluza 1.2 software package (Beckman Coulter Indianapolis, IN, USA). The positive cells were counted and their flowcytometric signal was compared with the signal of corresponding immunoglobulin isotypes [9].

Cell seeding and culture on the scaffold. Given the construct shape and size (Figure 1), we chose the suspension seeding method to improve cellular adhesion. Each scaffold in the study was placed in a conical tube containing 250 ml of cell suspension (30000 cells) and incubated in a humidified atmosphere of 95% air with 5% CO_2 at 37 C for 24h under agitation to allow the cells adhesion on the substrates. The next day each scaffold was transferred inside a 24-well plate and cultured in GM. After a week, half of the scaffolds stayed on in GM. In contrast, the other half were induced to osteogenic phenotype by adding an osteogenic differentiation medium (OM, StemPro™ Osteogenesis differentiation kit, Thermo Fisher Scientific). After 14 and 21 days of culture, all the scaffold/cell construct were sacrificed to carry on the experiments. At the end of colonization, we would have a biocompatible structure composed of titanium coated with bone matrix.

2.2. Titanium-biohybrid middle ear prostheses analyses

2.2.1. Cell proliferation and osteogenic differentiation

Adhesion and Proliferation Assay (WST). To monitor cell proliferation, we evaluated by the WST method the optical density at 1, 7, 14, and 21 days after the seeding of the hASCs on the scaffolds. Cell proliferation was evaluated with the Quick Cell Proliferation Colorimetric Assay Kit (Abcam, Waltham, MA, USA, #K301) according to the manufacturer's instructions. The assay is based on the degradation of the tetrazolium salt WST-1 to formazan by cellular mitochondrial dehydrogenase. The dye amount generated by the activity of dehydrogenase is directly proportional to the number of living cells. The formazan dye produced by viable cells can be quantified by measuring the absorbance of the dye solution at 450 nm. To exclude the signal from cells adhered to the plastic plates, the scaffolds were moved to new wells before the WST assay. hASCs cultured on scaffolds in GM and OM were incubated with 10% WST working solution for 2 h at 37 °C (95% air with 5% CO_2), and then the absorbance was read using a spectrophotometer.

RNA isolation and reverse transcriptase quantitative real-time PCR (qRT-PCR). To monitor the osteogenic differentiation, the gene expression of some known indicators of the osteoblast phenotype was tested on the constructs. To evaluate gene expression after 14 days from the induction of osteogenic differentiation, RNA was extracted from the constructs with GeneMATRIX KIT for RNA purification (Biosigma). The total RNA extracted was reverse-transcribed into cDNA using random hexamers and M-MLV Reverse Transcriptase, according to Laforenza et al. 2010 [7]. Quantitative real-time (RT-PCR) was performed in triplicate using 2 µL cDNA obtained as above, using specific primers from Qiagen: ALP (QT00012957), RUNX-2 (QT00020517), *COL1A1*(QT00037793), OSX (QT00213514), BGLAP (QT00232771), SMPD4 (QT00087353). Quantifast-SYBR Green PCR Kit (Qiagen) was used according to the manufacturer's instruction and qPCR was performed using StepOnePlus™ Real-Time PCR System (Applied Biosystems™). Cycling conditions: initial denaturation at 95 °C for 5 min; 40 cycles of denaturation at 95 °C for 30 s; annealing at 60 °C for 30 s, and elongation at 72 °C for 40 s. Melting curves were generated to identify the melting temperatures of specific products after the PCR run. The qPCR reactions were normalized against the expression of the housekeeping gene β2M gene (beta-2 micro-globulin, QT00088935, Qiagen, Hilden, Germany). Results of gene expression of differentiated cells on the scaffold were expressed as fold change versus expression of hASC on the scaffold after 14 days of culture in the growth medium (control).

2.2.2. Production of extracellular matrix

Immunofluorescence assay. The presence of collagen on the scaffold- which denotes the production of extracellular matrix- was demonstrated with an immunofluorescence assay to mark both phalloidin and Col1a1. After 21 days from seeding, the cells grown on scaffolds cultured in GM and OM were fixed with paraformaldehyde at 4% (PFA 4%) in PBS for 30 min. Cells were permeabilized with TRITON-X 0.4%, washed three times with PBS 1X, and incubated overnight at 4°C with the diluted (1:50) primary antibody against COL1A1 (PA1-26204, Thermo Fisher Scientific, Waltham, MA, USA). Thereafter, the scaffolds were washed three times with PBS 1X and incubated with a secondary antibody diluted 1:1000 (A-21207, Thermo Fisher Scientific) for 30 min at RT. Then, the

scaffolds were washed threetimes with PBS 1X and incubated with PHALLOIDIN (PHALLOIDIN Atto 488 Sigma) following the data sheet. Finally, the scaffolds were mounted with an anti-fading mounting solution (ProLong™ Gold Antifade Mountant Thermo Fisher Scientific) and kept at 4 °C until their visualization with the fluorescence microscope Nikon Eclipse 80i (Nikon, Tokyo, Japan).

SEM analysis. The presence of extracellular matrix on the construct was evaluated with scanning electron microscopy (SEM). After 21 days from differentiation, the constructs were washed with PBS and then fixed with glutaraldehyde 2.5% in 0.4 M of Sodium Cacodylate Buffer for 2 h. Then the constructs were washed with Sodium Cacodylate buffer for 30 min and dehydrated with graded ethanol series, starting from 50, 70, 90, and 100%. Microstructural characterization was performed with a high-resolution scanning electron microscope (SEM: EVO 40 SMART scanning electron microscope, Zeiss and TESCAN Mira 3 XMU) v at 20 kV. Two different SE and BSE analyses were performed. SE uses secondary electrons emitted by the affected material to obtain a high-resolution three-dimensional image, while BSE uses the interaction between the electrons and atomic nuclei of the analyzed sample to create a grayscale image. The samples were previously coated with carbon using a Cressington carbon coater 208c. SEM analyses were performed at Arvedi Laboratory, CISRiC (Centro Interdipartimentale di Studi e Ricerche per la Conservazione del Patrimonio Culturale), University of Pavia.
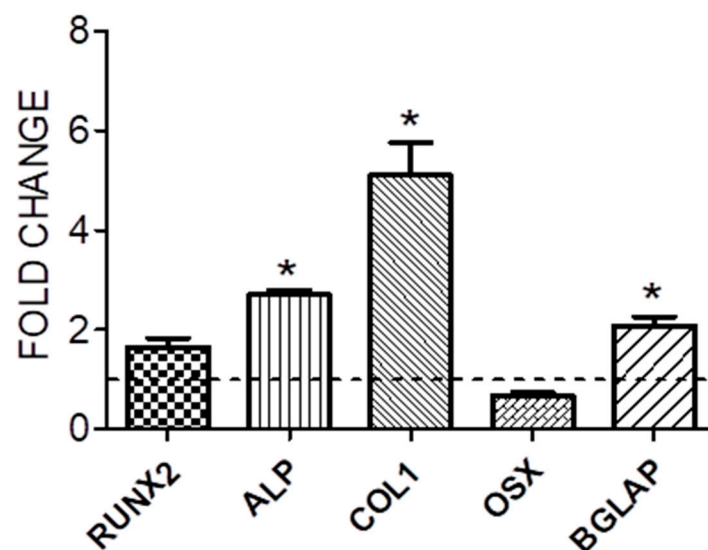
3. Results

3.1. Cell proliferation and osteogenic differentiation

Adhesion and proliferation assay. After 7 days from seeding, the osteogenic differentiation of 10 scaffolds was induced. The cells did not show a significative growth in the first week, but the numbers were steady. From day 14th, there was a remarkable increase of the optical density in cultured constructs cultured in GM, and a decreased signal from scaffolds cultured in OM, in line with the concept that cell differentiation inhibits cells proliferation (Figure 2).
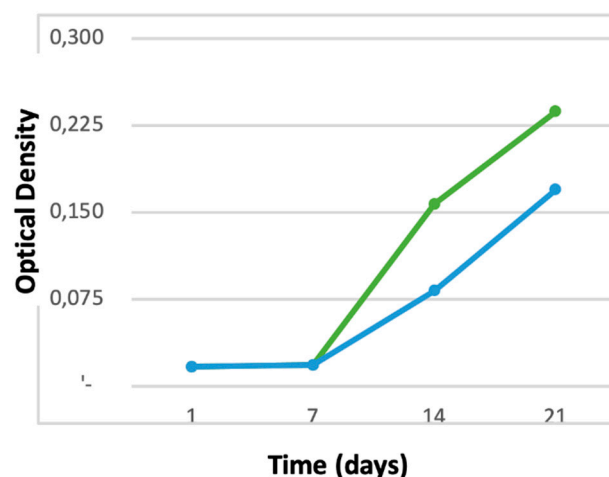
Figure 2. Optical density. The graphic represents the values of the optical density at 1, 7, 14, and 21 days after seeding, in growth medium (blue) and osteogenic differentiation medium (green). The differentiation of half scaffold starts from 7 days from seeding.

mRNA Expression. The mRNA expression of RUNX2, ALP, COL1A1, OSX, BGLAP, and SMPD4 was assessed by qRT-PCR in hASCs seeded on scaffold cultured in GM and OM. According to the melt curve plot, there was only one peak corresponding to a single amplicon, indicating the specificity of the PCR reaction. The qRT-PCR results of the *Alp, Runx2, Col1a1, Osx, Bglap,* and *Smpd4* were expressed as fold change versus the expression of hASC seeded on scaffold cultured in the absence of osteogenic medium (control). After 14 days, there was a significant increase in the expression of *Bglap, Smpd4, Col1a1,* and *Alp* (Figure 3).

Figure 3. Gene expression. Gene expression of hASCs seeded on the scaffold and cultured in the presence of osteogenic medium for 14 days. The gene expression results were expressed as fold change versus the expression of hASC seeded on the scaffold and cultured in the absence of an osteogenic medium (control). The dashed line represents control. Bars represent the mean ± S.E.M. of at least 2 different experiments each from different RNA extracts. *, $p \leq 0.05$ versus control. *ALP*, alkaline phosphatase; *OSX*, osterix; *BGLAP*, osteocalcin; *SMPD4*, Sphingomyelin Phosphodiesterase 4,.

3.2. Production of extracellular matrix

Immunofluorescence assay. The deposition of collagen (in red) on the scaffold cultured in OM was evidenced by the red coloration that was absent on the scaffold cultured in GM (Figure 4, A, and B respectively). This demonstrates that the cells were able to differentiate in an osteogenic lineage and to deposit bone matrix on the structure.
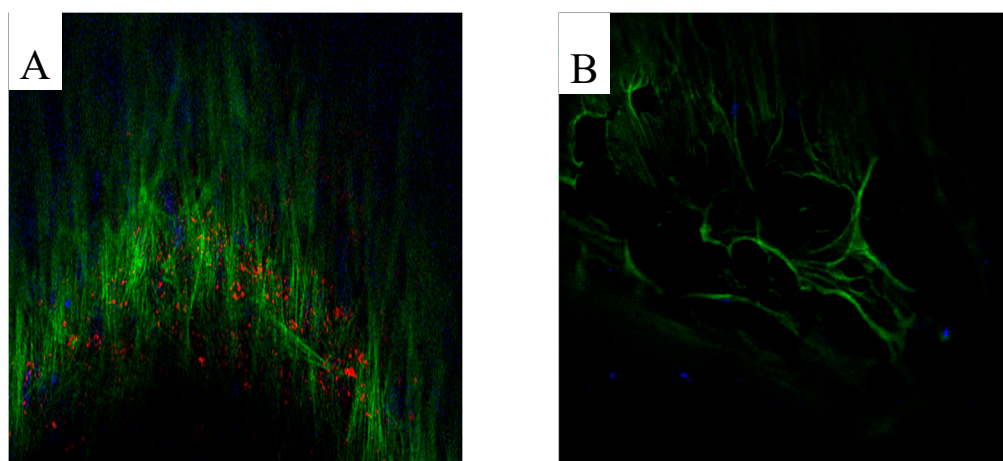

Figure 4. Immunofluorescence assay: (A) IF results of COL1A1 and PHALLOIDIN conducted on a scaffold colonized with hASC differentiated in osteoblasts, mag 20X; (B) IF results of COL1A1 and PHALLOIDIN conducted on a scaffold colonized with hASC cultured in GM, mag 20X. Cell nucleus, blue; phalloidin, green; COL1A1, red.

SEM analysis. SEM analysis showed the presence of many cells on both GM and OM-cultured scaffolds (Figure 5). The backscattered electrons detector (BSE, on the right) allowed us to visualize cells and their matrix: the matrix and the cells appeared dark, while the metallic scaffold appeared white (Figure 5, B, and D).
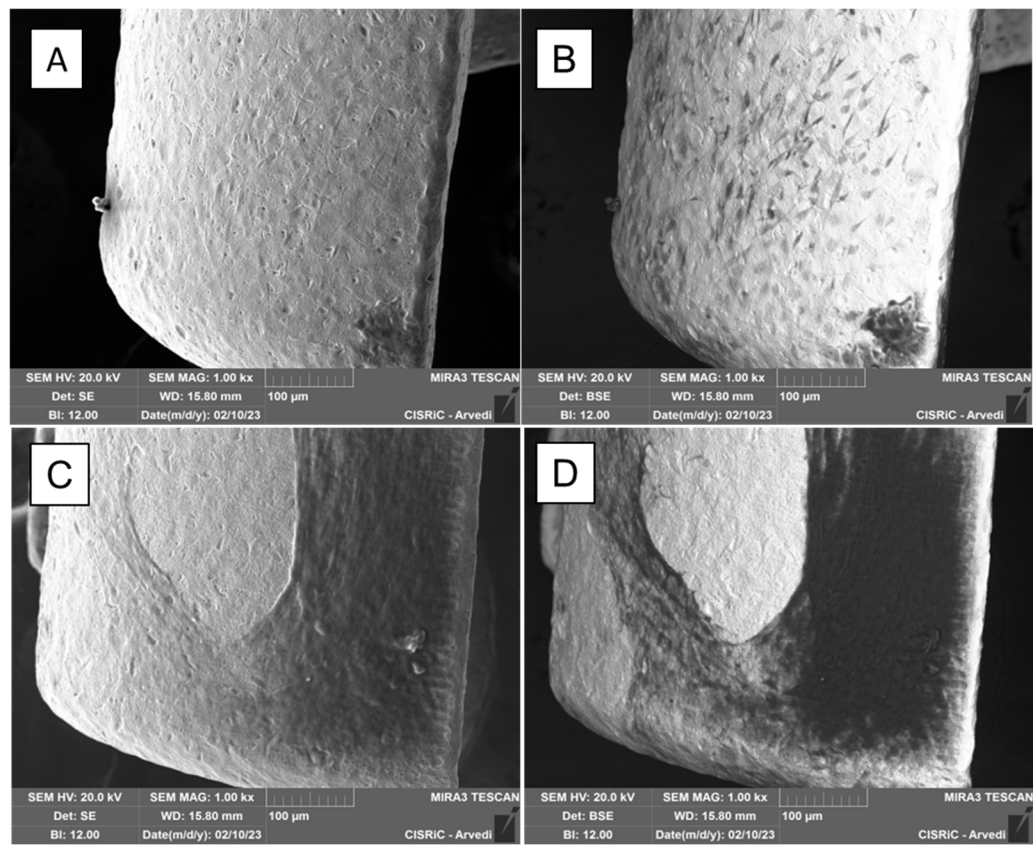
Figure 5. SEM images with scattered electrons detector (SE) and backscattered electrons detector (BSE) of the scaffold in GM (A and B) and in OM (C and D). With the BSE detector cells and matrix appeared dark, prosthesis white. It is evident that scaffolds cultured in the presence of osteogenic medium are richer in matrix (Figure 5 C and D). Mag.:1 kx**.**

At higher magnification (5000x) abundant matrix is secreted by the hASCs differentiated in osteoblasts on the prosthesis (Figure 6).
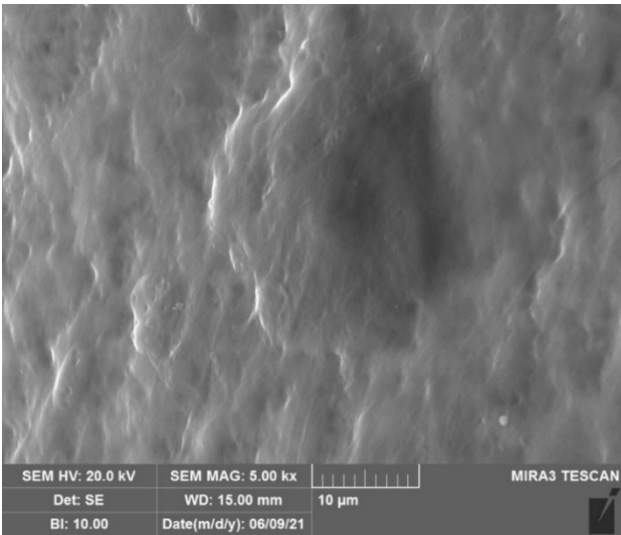
Figure 6. SEM analysis of matrix on the scaffold. SEM analysis with SE detector of abundant matrix secreted by hASC differentiated in osteoblasts on the scaffold. (Mag.: 5.00 kx)**.**

4. Discussion

ME surgery outcomes are undeniably influenced by the pre-existing conditions of the tympanic cavity and the clinical behavior of ME diseases. This tight clinical-surgical correlation has stimulated the development of many strategies for disease eradication and hearing rehabilitation over the years, including approaches that bypass ME sound conduction [10][11]. On the other side, among the surgical solutions intended to restore a mechano-acoustic coupling between the tympanic membrane and the stapes footplate, the synthetic ME prostheses still play a prominent role in the modern ME otosurgery, since they mimic the natural mechanics of sound wave transmission at this level. Titanium is reported to be an excellent material for synthetic ME prosthesis because of its intrinsic properties, it is light, rigid, non-ferromagnetic, easy to hand during surgery, and it is a good sound wave conductor. However, this material presents a significant drawback shared by all synthetic materials currently in use for ME reconstruction, it can be rejected by the organism of the host. This phenomenon is known as extrusion. Specifically, host tissues interact with the surface of the synthetic implant inducing foreign body response and inflammation [12]. Foreign body inflammatory response and consequent prosthesis extrusion have an important negative impact on the long-term outcomes of the ossiculoplasty [5]. On the contrary, it has been observed that extrusion does not occur when biological materials are used [13]. Tissue engineering studies who focus on improving biointegration and on preserving acoustic performance are starting to appear in literature [5,6,14]. To the best of our knowledge, there is no record of ossicular replacement biohybrid prosthesis made up of titanium enveloped in bone matrix and living cells. Our experimental in vitro results represent the first feasibility study on this topic. The objective is to obtain a biohybrid device able to lowdown the risk of extrusion and to maintain the intrinsic acoustic properties of conventional titanium prosthesis. Experimental data show that hASC can adhere and proliferate on the scaffolds represented by titanium prostheses in use in our otosurgical department. Cells began to proliferate one week after seeding following a period of adaptation to the titanium surface. It is possible that an increase in the number of cells is not initially detectable because an equilibrium is reached between cells proliferation and apoptosis. The proliferation rate of hASCs on scaffolds cultured in osteogenic medium was slower compared to those in growth medium: this is due to the fact that cells tend to inhibit proliferation in favor of differentiation. Gene expression was analyzed 14 days after differentiation induction both in GM and in OM. In particular, we analyzed the expression of the following genes indicative of bone differentiation: Alp, Runx2, Col1a1, Osx, and Bglap. Alp has two principal roles during osteogenic differentiation. It is an important player in the first phase of differentiation and in bone mineralization, so it is considered both an early and late marker of differentiation. Runx2 is an early marker of bone differentiation since it is the first transcription factor required for determination of the osteoblast lineage and its levels decrease as the osteoblasts mature: this is the reason why there are no differences between the cells in GM and those in OM. Osx regulates osteoblast differentiation and inhibits osteoblasts mature markers like Col1a1 and Bglap. Col1a1 is associated with osteogenic differentiation and mineralization, while Bglap is involved in bone remodeling, by calcium binding and metabolism, and energy metabolism on osteoblasts [15,16]. The gene expression data show that the cells are in the first phase of bone differentiation: there is a significant increase of Alp, Col1a1, and Bglap, but an unmodified expression of Runk2. In agreement with the literature, Osx expression does not show any modification compared to controls because it is a late marker of the differentiation [16]. We performed immunofluorescence assay to mark both phalloidin and Col1a1. Phalloidin stains polymerized form of actin (F-actin), the main component of the cytoskeleton, while Col1a1 is the main component of Collagen Type I, the most abundant form of collagen in human body. Collagen is the main protein of connective tissues, including bone tissue. Phalloidin staining shows that the cells were viable at the time of fixation, while the presence of Col1A1 in OM and its absence in GM indicates the beginning of differentiation and deposition of the bone matrix in OM. Moreover, SEM showed buildup of matrix on scaffolds cultured in OM. All in

all, OM has demonstrated to be the most appropriate tool for our purposes. The preliminary data derived from our work seem encouraging. However, corroboration from a bigger sample size and comparison with other titanium-prothesis models are required to validate our results. In our opinion, the evidence supported by this preliminary study should be implemented with functional investigations on the sound transmission properties of biohybrid products. Finally, we advocate further research to improve biohybrid prostheses manufacturing. An example could be the use of three-dimensional (3D) printing technology which has been widely documented in otoneurosurgery [17,18]. We can speculate that the production of ossicular replacement biohybrid prostheses could be optimized by introducing devices made-up of titanium surrounded by a 3D-printed self-absorbable superstructure facilitating the scaffold coating by hASC, as a sort of bone transplantation.

5. Conclusions

To the best of our knowledge, this is the first feasibility study exploring a biohybrid prosthesis composed of titanium surrounded by bone matrix as a possible tissue engineering option for fabricating ME ossicle replacements. Our experience seems promising, in future animal studies will be required evaluate the percentage of device expulsion and to test their in vivo application. Furthermore, clinical trials should be run in the attempt to establish in the surgical practice these biohybrid protheses combining the advantages of both titanium and biologic tissues.

References

1. Kim, H.; Ha, J.; Choo, O.-S.; Park, H.; Choung, Y.-H. Which Is Better for Ossiculoplasty following tympanomastoidectomy: Polycel® or Titanium? *Ann Otol Rhinol Laryngol* **2023**, 000348942311599, doi:10.1177/00034894231159969.

2. Faramarzi, M.; Roosta, S.; Faramarzi, A.; Khera, M. Comparison of partial vs. total ossicular chain reconstruction using titanium prosthesis: a retrospective cohort study. *Eur Arch Otorhinolaryngol* **2023**, *280*, 3567-3575, doi: 10.1007/s00405-023-07849-6.

3. Coffey, C.S.; Lee, F.; Lambert, P.R. Titanium versus nontitanium prostheses in ossiculoplasty. *Laryngoscope* **2008**, *118*, 1650–1658, doi:10.1097/MLG.0b013e31817bd807.

4. Kortebein, S.; Russomando, A.C.; Greda, D.; Cooper, M.; Ledbetter, L.; Kaylie, D. Ossicular chain reconstruction with titanium prostheses: a systematic review and meta-analysis. *Otol Neurotol* **2023**, *44*, 107–114, doi:10.1097/MAO.0000000000003772.

5. Danti, S.; Stefanini, C.; D'Alessandro, D.; Moscato, S.; Pietrabissa, A.; Petrini, M.; Berrettini, S. Novel biological/biohybrid prostheses for the ossicular chain: fabrication feasibility and preliminary functional characterization. *Biomed Microdevices* **2009**, *11*, 783–793, doi:10.1007/s10544-009-9293-9.

6. Danti, S.; D'Alessandro, D.; Pietrabissa, A.; Petrini, M.; Berrettini, S. Development of tissue-engineered substitutes of the ear ossicles: PORP-shaped poly(propylene fumarate)-based scaffolds cultured with human mesenchymal stromal cells. *Biomed Mater Res A* **2010**, *92*, 1343–1356, doi:10.1002/jbm.a.32447.

9

7. Laforenza, U.; Miceli, E.; Gastaldi, G.; Scaffino, M.F.; Ventura, U.; Fontana, J.M.; Orsenigo, M.N.; Corazza, G.R. Solute Transporters and Aquaporins Are Impaired in Celiac Disease. *Biology of the Cell* **2010**, *102*, 457–467, doi:10.1042/BC20100023.

8. Caliogna, L.; Bina, V.; Botta, L.; Benazzo, F.M.; Medetti, M.; Maestretti, G.; Mosconi, M.; Cofano, F.; Tartara, F.; Gastaldi, G. Osteogenic potential of human adipose derived stem cells (HASCs) seeded on titanium trabecular spinal cages. *Sci Rep* **2020**, *10*, 18284, doi:10.1038/s41598-020-75385-y.

9. Huang, X.; Das, R.; Patel, A.; Duc Nguyen, T. Physical stimulations for bone and cartilage regeneration. *Regen Eng Transl Med* **2018**, *4*, 216–237, doi:10.1007/s40883-018-0064-0.

10. Canzi, P.; Berrettini, S.; Albera, A.; Barbara, M.; Bruschini, L.; Canale, A.; Carlotto, E.; Covelli, E.; Cuda, D.; Dispenza, F.; et al. Current trends on subtotal petrosectomy with cochlear implantation in recalcitrant chronic middle ear disorders. *Acta Otorhinolaryngol Ital* **2023**, *43*, S67–S75, doi:10.14639/0392-100X-suppl.1-43-2023-09.

11. Canzi, P.; Avato, I.; Beltrame, M.; Bianchin, G.; Perotti, M.; Tribi, L.; Gioia, B.; Aprile, F.; Malpede, S.; Scribante, A.; et al. Retrosigmoidal placement of an active transcutaneous bone conduction implant: surgical and audiological perspectives in a multicentre study. *Acta Otorhinolaryngol Ital* **2021**, *41*, 91–99, doi:10.14639/0392-100X-N0609.

12. Kong, J.S.; Jeong, C.Y.; Shim, M.J.; Kim, W.J.; Yeo, S.W.; Park, S.N. Comparative study of new autologous material, bone-cartilage composite graft, for ossiculoplasty with Polycel ® and Titanium. *Clin Otolaryngol* **2018**, *43*, 434–439, doi:10.1111/coa.12987.

13. Van Rompaey, V.; Farr, M.R.B.; Hamans, E.; Mudry, A.; Van De Heyning, P.H. Allograft tympanoplasty: a historical perspective. *Otol Neurotol* **2013**, *34*, 180–188, doi:10.1097/MAO.0b013e31826bf16d.

14. D'Alessandro, D.; Danti, S.; De Vito, A.; Forli, F.; Bruschini, L.; Berrettini, S. Histologic characterization of human ear ossicles for the development of tissue-engineered replacements. *Otol Neurotol* **2012**, *33*, 1458–1468, doi:10.1097/MAO.0b013e31826a527d.

15. Subramaniam, M.; Pitel, K.S.; Withers, S.G.; Drissi, H.; Hawse, J.R. TIEG1 enhances Osterix expression and mediates its induction by TGFβ and BMP2 in osteoblasts. *Biochem Biophys Res Commun* **2016**, *470*, 528–533, doi:10.1016/j.bbrc.2016.01.112.

16. Caliogna, L.; Bina, V.; Brancato, A.M.; Gastaldi, G.; Annunziata, S.; Mosconi, M.; Grassi, F.A.; Benazzo, F.; Pasta, G. The role of PEMFs on bone healing: an in vitro study. *IJMS* **2022**, *23*, 14298, doi:10.3390/ijms232214298.

17. Canzi, P.; Avato, I.; Marconi, S.; Del Maestro, M.; Lucifero, A.G.; Magnetto, M.; Carlotto, E.; Auricchio, F.; Luzzi, S.; Benazzo, M. A 3D printed custom-made mask model for frameless neuronavigation during retrosigmoid craniotomy. A preclinical cadaveric feasibility study. *Ann Ital Chir* **2020**, *91*, 526-533.

18. Canzi, P.; Magnetto, M.; Marconi, S.; Morbini, P.; Mauramati, S.; Aprile, F.; Avato, I.; Auricchio, F.; Benazzo, M. New frontiers and emerging applications of 3D printing in ENT surgery: a systematic review of the literature. *Acta Otorhinolaryngol Ital* **2018**, *38*, 286–303, doi:10.14639/0392-100X-1984.